EVALUATION OF A DIFFUSION/TRAPPING MODEL FOR HYDROGEN INGRESS IN HIGH STRENGTH ALLOYS

November 1989

Annual Report
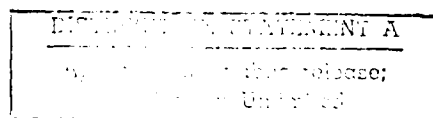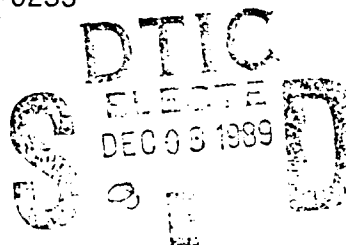
By: Bruce G. Pound
        Materials Research Laboratory

DTIC
ELECTE
DEC 0 6 1989

SRI International

REPORT DOCUMENTATION PAGE

1a REPORT SECURITY CLASSIFICATION	1b RESTRICTIVE MARKINGS
Unclassified	

2a SECURITY CLASSIFICATION AUTHORITY	3 DISTRIBUTION/AVAILABILITY OF REPORT
	Approved for public release – distribution
2b DECLASSIFICATION/DOWNGRADING SCHEDULE	unlimited. Reproduction in whole or part is permitted for any purpose of the U.S. Gov't.

4 PERFORMING ORGANIZATION REPORT NUMBER(S)	5 MONITORING ORGANIZATION REPORT NUMBER(S)
PYU-1962	

6a NAME OF PERFORMING ORGANIZATION	6b OFFICE SYMBOL (If applicable)	7a NAME OF MONITORING ORGANIZATION
SRI International		

6c ADDRESS (City, State, and ZIP Code)	7b ADDRESS (City, State, and ZIP Code)
333 Ravenswood Avenue Menlo Park, CA 94025-3493	

8a NAME OF FUNDING/SPONSORING ORGANIZATION	8b OFFICE SYMBOL (If applicable)	9 PROCUREMENT INSTRUMENT IDENTIFICATION NUMBER
Office Of Naval Research		N00014-86-C0233

8c ADDRESS (City, State, and ZIP Code)	10 SOURCE OF FUNDING NUMBERS			
	PROGRAM ELEMENT NO	PROJECT NO	TASK NO	WORK UNIT ACCESSION NO
Metallic Materials, Code 1131M 800 N. Quincy Street Arlington, VA 22217-5000				

11 TITLE (Include Security Classification)
Evaluation of a Diffusion/Trapping Model for Hydrogen Ingress in High Strength Alloys (Unclassified)

12 PERSONAL AUTHOR(S)
Pound, Bruce G.

13a TYPE OF REPORT	13b TIME COVERED	14 DATE OF REPORT (Year Month Day)	15 PAGE COUNT
Annual-Technical	FROM 88Nov. TO 89Nov.	89 Nov. 17	

16 SUPPLEMENTARY NOTATION

17 COSATI CODES			18 SUBJECT TERMS (Continue on reverse if necessary and identify by block number)
FIELD	GROUP	SUB-GROUP	Inconel 718, 18Ni maraging steel, Incoloy 925, Titanium, Hydrogen ingress, Diffusion/trapping model, Hydrogen Trapping.

19 ABSTRACT (Continue on reverse if necessary and identify by block number)

The ingress of hydrogen in three precipitation-hardened alloys (Inconel 718, Incoloy 925, and 18Ni maraging steel) and titanium (pure and grade 2) was studied using a potentiostatic pulse technique. Anodic current transients were obtained for these materials in an acetate buffer (1 mol L^{-1} HAc/1 mol L^{-1} NaAc where Ac = acetate). The data for the Ni-containing alloys and Ti grade 2 were shown to fit a diffusion/trapping model under interface control, and values were determined for the irreversible trapping constants (k) and the flux of hydrogen into the alloys. The absence of hydrogen ingress in the case of pure titanium indicates that the surface oxide is an effective barrier to hydrogen entry.

The density of irreversible trap defects in Inconel 718 and Incoloy 925 was calculated from k and found to be in excellent agreement with the concentration of NbC and TiC particles, respectively. Accordingly, these particles are considered to be the

20 DISTRIBUTION/AVAILABILITY OF ABSTRACT	21 ABSTRACT SECURITY CLASSIFICATION
☒ UNCLASSIFIED/UNLIMITED ☐ SAME AS RPT ☐ DTIC USERS	Unclassified

22a NAME OF RESPONSIBLE INDIVIDUAL	22b TELEPHONE (Include Area Code)	22c OFFICE SYMBOL
A. J. Sedriks	(202) 696-4401	1131M

DD FORM 1473, 84 MAR   83 APR edition may be used until exhausted   SECURITY CLASSIFICATION OF THIS PAGE
All other editions are obsolete

predominant irreversible types of trap in the respective alloys. The maraging steel was characterized by two trapping constants; one appears to be associated with quasi-irreversible traps that saturate, leaving only irreversible traps. These irreversible traps, with some uncertainty, appear to be TiC particles on the basis of the trap density obtained from k.

Two values of k were also obtained for Ti grade 2, depending on the level of hydrogen present in the metal. The density of irreversible traps calculated from k for low hydrogen levels correlates moderately well with the concentration of interstitial nitrogen. This correlation suggests that the principal irreversible traps may be the nitrogen, but grain boundaries are another possibility. The additional trapping constant obtained for high hydrogen levels is thought to be associated with the formation of hydrides.

The irreversible trapping constants for the three nickel-containing alloys and titanium grade 2 are consistent with their relative susceptibilities to hydrogen embrittlement, with the highest value for the maraging steel, followed in order by those for the Inconel and then the Incoloy and titanium grade 2. Moreover, a comparison of the trapping constants for these alloys with those for 4340 steel and two other nickel-base alloys (Monel K-500 and MP35N) indicates that a strong correlation exists between hydrogen embrittlement susceptibility and trapping capability over the full range of these alloys.

Accession For		
NTIS GRA&I	☒	
DTIC TAB	☐	
Unannounced	☐	
Justification		
By		
Distribution/		
Availability Codes		
Dist	Avail and/or Special	
A-1		

CONTENTS

LIST OF FIGURES

iv

LIST OF TABLES

INTRODUCTION

Hydrogen embrittlement can restrict the use of various metals and alloys in aqueous environments. The degradation of mechanical properties as a result of hydrogen ingress is of particular concern in high-strength alloys. Local interactions between the hydrogen and heterogeneities in the microstructure initiate the series of events leading to failure. Accordingly, a knowledge of the hydrogen interaction with heterogeneities in different alloys should contribute to an understanding of the susceptibility of high strength alloys to hydrogen embrittlement.

The structural heterogeneities are potential trapping sites for the diffusing hydrogen, and the nature of the interaction of hydrogen with these trap sites affects the resistance of the alloy to hydrogen embrittlement. Traps with both a high binding energy and a high specific saturability (number of hydrogen atoms bound per unit trap site) for hydrogen are thought to be the most conducive to hydrogen embrittlement.[1-3] The accumulation of hydrogen at second-phase particles and precipitates is generally considered to promote microvoid initiation via the fracture of particles or the weakening of particle-matrix interfaces. In contrast, metals containing a high density of well-distributed strong traps (high binding energy) that have a low specific saturability should exhibit little susceptibility to embrittlement. Therefore, identifying the dominant types of traps is crucial to determining the susceptibility of an alloy to hydrogen embrittlement.

By using a model developed[4] to represent the diffusion and trapping of hydrogen atoms, it is possible to identify the dominant types of traps in metals and alloys. The model is used in conjunction with a potentiostatic pulse technique and directly provides information on trapping characteristics that is not available from other methods. The technique and model have previously been applied to iron,[5] a high-strength steel (AISI 4340), and two high-strength nickel-base alloys (Monel K500 and MP35N).[6]

The application of the pulse technique and diffusion/trapping model has now been extended to a group of precipitation-hardened nickel-containing alloys (Inconel 718, Incoloy 925, and 18Ni maraging steel) and titanium (pure and grade 2). The objective was to obtain the hydrogen ingress and trapping characteristics for a range of microstructures and so identify the dominant type of irreversible trap in different alloys. Thus, the data obtained from the hydrogen ingress model is used to compare the trapping capability of the individual alloys and thereby provide a basis for explaining differences in the resistance of these alloys to hydrogen embrittlement.

1

EXPERIMENTAL PROCEDURE

The composition of each alloy was provided by the manufacturer and is given in Table 1. The titanium specimen was 99.99% pure.

Table 1
ALLOY COMPOSITION
(wt %)

Element	Inconel 718	Incoloy 925	18Ni Maraging Steel	Ti Grade 2
Al	0.60	0.30	0.13	
B	0.003		0.003	
C	0.03	0.02	0.009	0.021
Co	0.16		9.15	
Cr	18.97	22.20	0.06	
Cu	0.04	1.93	0.11	
Fe	16.25	28.96	bal	0.17
Mn	0.10	0.62	0.01	
Mo	3.04	2.74	4.82	
Ni	54.41	40.95	18.42	
P	0.009		0.004	
S	0.002	0.001	0.001	
Si	0.11	0.17	0.04	
Ti	0.98	2.11	0.65	bal
Other	5.30 Nb+Ta		0.05 Ca 0.01 W 0.02 Zr	0.007 N 0.16 O < 0.0050 H

All the materials were supplied in the form of 1.27-cm rod and were used in the as-received condition. The yield strength and the particle characteristics of each alloy as received are given in Table 2.

Table 2
CHARACTERISTICS OF ALLOYS

Alloy	Yield Strength (ksi)	Particle Characteristics		
		Type	Dimension (μm)	Concentration m^{-3}
Inconel 718	179.6	NbTi(CN)	7.8	2.2×10^{13}
Incoloy 925	109.9	TiC	2.9	4.1×10^{13}
18Ni Steel	283.4	Ti(CN)	3.4	1.1×10^{13}
Ti Grade 2	55.1	-	-	-

The nickel-containing alloys develop micrometer-size MC-type carbides (where M is the metallic component). In the case of Inconel 718, the carbide has been identified as niobium carbide with some titanium and titanium nitride dissolved in it or NbTi(CN).[7] Large MC carbide particles have also been identified in Incoloy 901,[8] which is similar in titanium content to the 925 alloy, and maraging steels can form carbides and carbo-nitrides, Ti(CN).[9,10] All the specimens used in this study were found to contain large particles randomly distributed, and an energy dispersive x-ray analysis showed the particles to contain titanium with niobium also present in the Inconel. The characteristic dimension (Table 2) of these particles was determined as the mean of the linear dimensions in the exposed plane. The concentration of particles was calculated on the basis of a spherical shape, with the radius taken as half the characteristic dimension. In the case of the maraging steel, there was a considerable distribution in the particle size and some degree of uncertainty in the particle concentration.

Details of the electrochemical cell and instrumentation have been given previously.[6] The test electrodes of each alloy consisted of a 5-cm length of rod press-fitted into a Teflon sheath so that only the planar end surface was exposed to the electrolyte. The surface was polished with SiC paper followed by 0.05-μm alumina powder. The same sample of each alloy was used throughout the study, but it was repolished before each experiment to remove metal previously exposed to absorbed hydrogen. The electrolyte was an acetate buffer (1 mol L^{-1} acetic acid/1 mol L^{-1} sodium acetate) containing 15 ppm As_2O_3 as a hydrogen entry promoter. The electrolyte was deaerated with argon for 1 hour before measurements began and throughout data acquisition. The potentials were measured with respect to a saturated calomel electrode (SCE). All tests were performed at

$22 \pm 2°C$.

The pulse technique has been described previously.[4-6] Briefly, the test electrode is charged with hydrogen at a constant potential (E_c) for a time (t_c), after which the potential is stepped to a more positive value, E_A (10 mV negative of the open-circuit potential). The charging time was varied from 0.5 s to 50 s for each E_c. Anodic current transients with a charge q_a were obtained for each charging time over a range of overpotentials ($\eta = E_c - E_{oc}$). The open-circuit potential (E_{oc}) of the test electrode was sampled immediately before each charging time and was also used to monitor the stability of the surface film; reduction of the film was evident from a progressive shift of E_{oc} to more negative values with each t_c at a sufficiently high charging potential.

ANALYSIS

DIFFUSION/TRAPPING MODEL

Typical anodic current transients for a nickel-containing alloy (Inconel 718) and titanium (grade 2) are shown in Figures 1 and 2. The diffusion/trapping model used to analyze the anodic transients has been developed for two cases under conditions imposed by the pulse technique: (1) diffusion control, in which the rate of hydrogen ingress is controlled by diffusion in the bulk metal; and (2) interface control, in which the rate of ingress is controlled by the flux across the interface.[4] Analysis of the transients assuming diffusion control gave trapping parameters that changed with t_c and E_c, indicating that this limiting case was not appropriate to any of the alloys studied.

The data were therefore analyzed in terms of the interface control model, for which the total charge passed out is given in nondimensional form by[4]

$$Q'(\infty) = \sqrt{R}\{1 - e^{-R}/\sqrt{(\pi R)} - [1 - 1/(2R)]erf\sqrt{R}\} \tag{1}$$

The nondimensional terms are defined by $Q = q/[FJ\sqrt{(t_c/k_a)}]$ and $R = k_a t_c$ where q is the dimensionalized charge in C cm^{-2}, F is the Faraday constant, J is the ingress flux in mol cm^{-2} s^{-1}. The charge $q'(\infty)$ corresponding to $Q'(\infty)$ is equated to q_a. k_a is an apparent trapping constant measured for irreversible traps in the presence of reversible traps and is given by $k/(1 + K_r)$, k is the irreversible trapping constant, and K_r is an equilibrium constant for reversible traps.

The adsorbed charge (q_{ads}) was negligible in all cases, and so q_a was assumed to be associated entirely with absorbed hydrogen. Data for q_a could be fitted to Eq. (1) to obtain values of k_a and J such that the ingress flux was constant over the range of charging times and k_a was essentially independent of charging potential. As discussed previously,[6] the data analysis was restricted to charging times from 10 s to 40 s.

The values of k_a and J can be used to calculate the charge (q_T) irreversibly trapped and the ingress charge given nondimensionally by
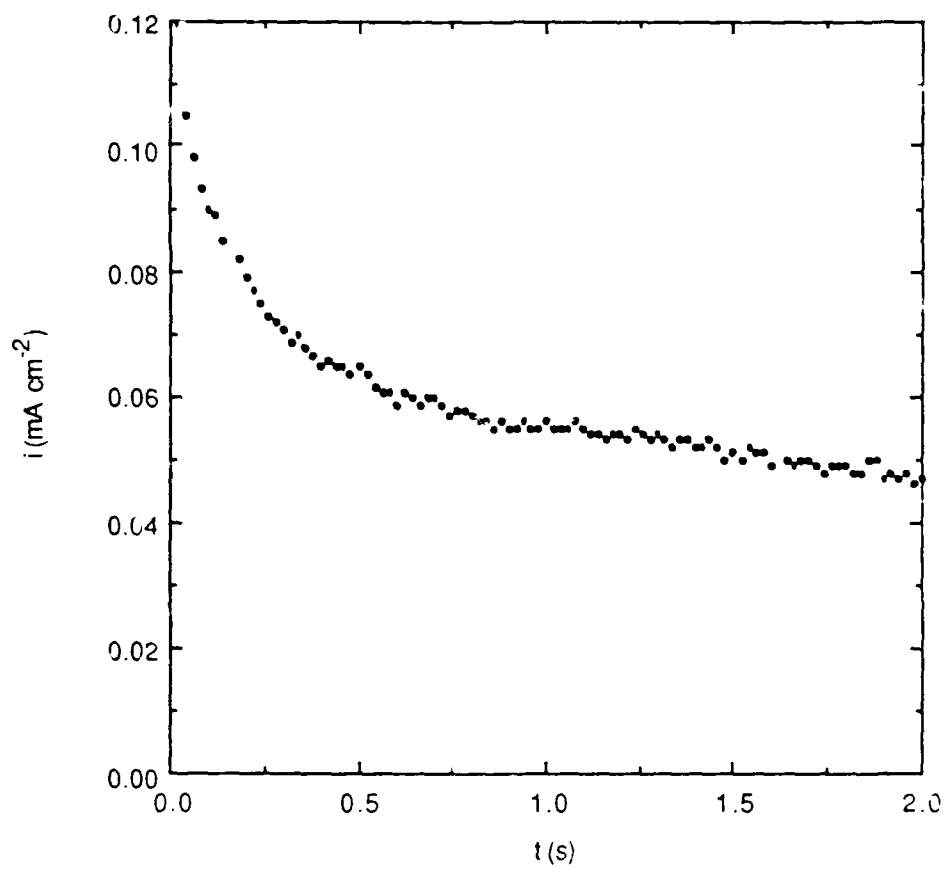
Figure 1. Anodic transient for Inconel 718 in acetate buffer.
t_c = 10 s; E_c = -0.671 V (SCE).

The full transient is not shown.

RA-1962-19

6

RA-1962-20

Figure 2. Anodic transient for titanium grade 2 in acetate buffer.
t_c = 15 s; E_c = -0.742 V (SCE).

The full transient is not shown.

$$Q_T = [\sqrt{R} - 1/(2\sqrt{R})]\text{erf}\sqrt{R} + e^{-R}/\sqrt{\pi} \tag{2}$$
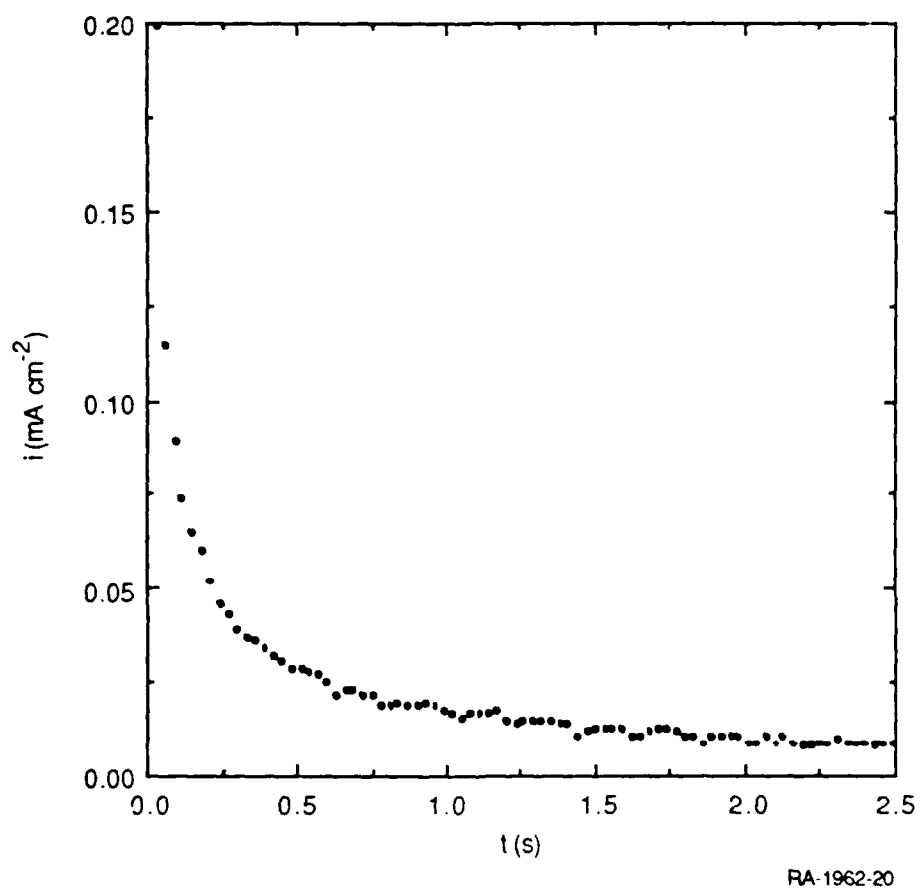
The charge associated with the entry of hydrogen into the metal (q_{in}) can be determined from its nondimensional form of $Q_{in} = \sqrt{R}$ by using the derived value of k_a. The data for q_{in}, q_T, and the cathodic charge (q_c) can then used to obtain two ratios: (1) q_T/q_{in}, corresponding to the fraction of hydrogen in the metal that is trapped; and (2) q_{in}/q_c, representing the fraction of charge associated with hydrogen entry during the charging step. The ratio q_T/q_{in} is independent of potential because each component has the same dependence on flux, whereas q_{in}/q_c generally exhibits some variation with potential.

EVALUATION OF TRAP DENSITY

The density of irreversible traps (N_i) can be obtained from the trapping constant (k) on the basis of a knowledge of the dimensions of the potential traps and the hydrogen diffusivity. The trapping constant can be used to calculate the density of irreversible trap particles by using a model based on spherical traps of radius d:[5]

$$k = 4\pi d^2 N_i D_L/a \tag{3}$$

where D_L is the lattice diffusivity of hydrogen and a is the diameter of the metal atom. The apparent diffusivity (D_a) is given by $D_L/(1 + K_r)$,[6] and so the irreversible trapping constant (k) can be expressed as $k_a D_L/D_a$. Therefore, the trap density can be represented in terms of the apparent trapping constant:

$$N_i = k_a a/(4\pi d^2 D_a) \tag{4}$$

Although the apparent diffusivity is needed to calculate N_i, it is evident that the diffusivity (D_L) for the trap-free "pure" metal or alloy is not required. The calculation of N_i also involves the trap radius (d), and the evaluation of d presupposes a knowledge of potential irreversible traps. Thus, in calculating N_i from k_a, the microstructure of the alloy must be characterized in terms of the dimensions of its heterogeneities. The dominant irreversible trap can then be identified by comparing the trap density with the concentrations of potential traps in the alloy.

The assumption of spherical traps in the above model is an approximation in most cases, and

8

it is possible that models for specific trap geometries will lead to more accurate values of the trap density. In alloys where the concentrations of potential traps have distinct ranges, the incorporation of a more applicable trap geometry will make little difference in identifying the principal traps. However, more specific models may be necessary to resolve cases where the concentration ranges of traps are close and even overlap.

RESULTS

INCONEL 718

The values of k_a and J for two tests are given in Table 3. In both cases, k_a is independent of overpotential, as is required for the diffusion/trapping model to be valid, since the traps are assumed to be unperturbed by electrochemical variables and remain unsaturated. The mean value of k_a is 0.031 ± 0.002 s^{-1}. The flux in general does not exhibit a significant change with overpotential. However, a small decrease occurring at -0.25 V is probably related to instability of the oxide at high cathodic potentials.

With the above value for k_a and the appropriate value of J used in Eq. (1), q_a was calculated for the full range of charging times (0.5 s to 40 s) and compared with the corresponding experimental results. The two sets of data for the Inconel charged at $\eta = -0.15$ V in test 2 are shown in Figure 3. The close fit between them is typical for each overpotential and illustrates the independence of both k_a and J with respect to t_c.

The values of k_a and J were used to calculate the charge irreversibly trapped (q_T) and the ingress charge (q_{in}), and the charge ratios (q_T/q_{in} and q_{in}/q_c) were then obtained. The charge ratios are shown as a function of t_c in Figures 4 and 5. The fraction of hydrogen trapped (q_T/q_{in}) is found empirically to vary approximately linearly with $\sqrt{t_c}$, although the reason for this relatively simple dependence is not apparent from the more complex relationship between q_T and t_c. Some deviation from linearity occurs at long charging times, which is to be expected in view of the quite different t_c dependence of q_T and q_{in}.

In contrast to q_T/q_{in}, the fraction of hydrogen entering the metal (q_{in}/q_c) exhibits a linear dependence on t_c. However, the change in q_{in}/q_c decreases with increasing overpotential to the extent that the ratio becomes essentially constant with t_c. The q_{in}/q_c ratio itself decreases with increasing overpotential (Figure 6), which indicates a loss of charging efficiency that is probably due to an increasing rate of chemical recombination of hydrogen ($\propto \theta^2$) relative to the rate of hydrogen entry ($\propto \theta$).

Figure 3. Comparison of experimental and calculated anodic charge data for Inconel 718 in acetate buffer.

$E_c = -0.671$ V (SCE).

11
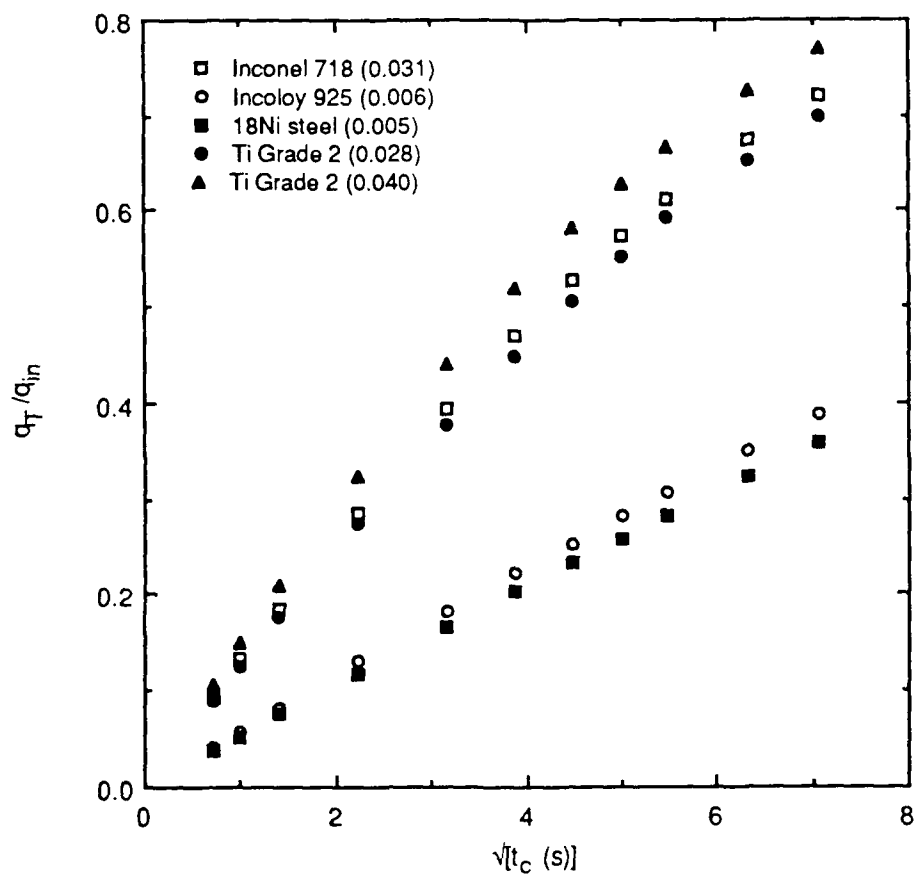
RA-1962-22

Figure 4. Dependence of q_T/q_{in} on charging time for each alloy.

The apparent rate constants are given in parentheses
for the particular alloy.

12
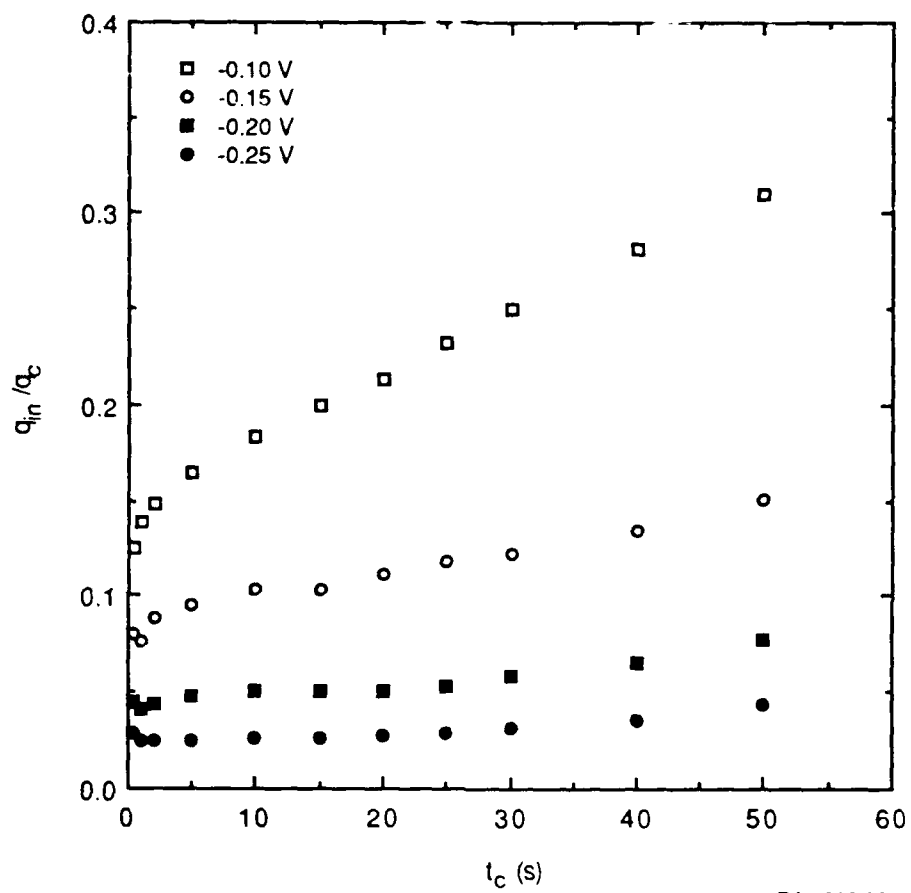
RA-1962-23

Figure 5. Dependence of q_{in}/q_c on charging time for Inconel 718 at various overpotentials.

13
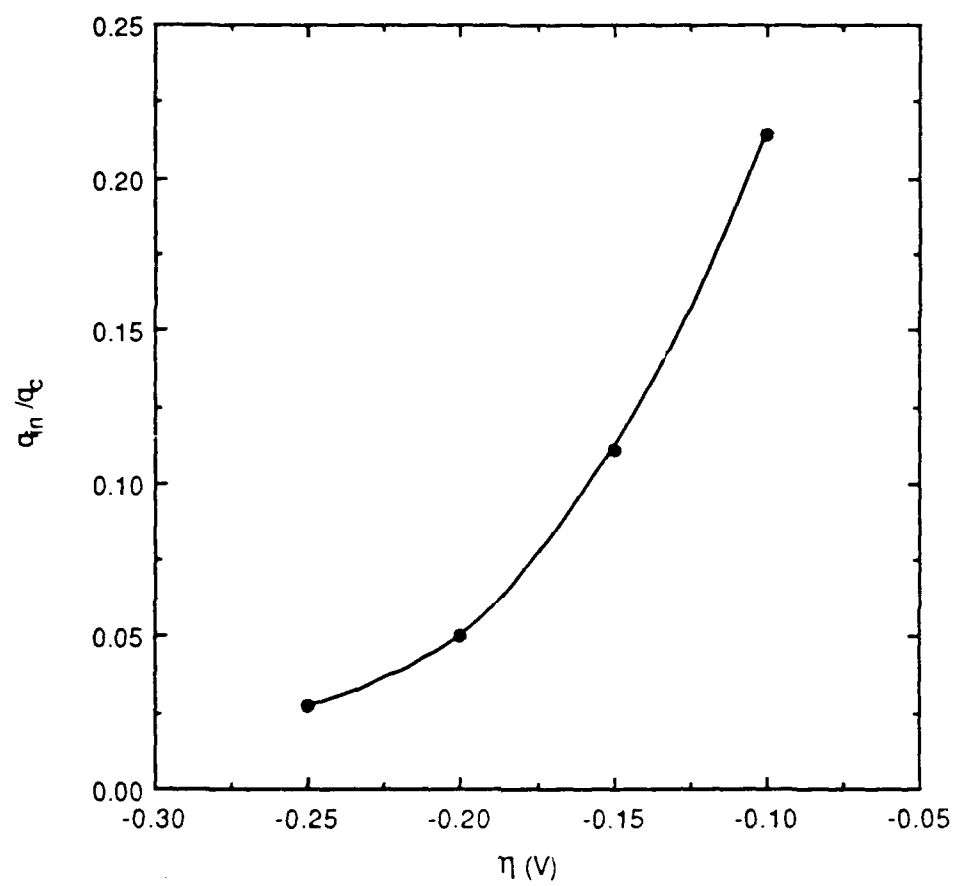
RA-1962-24

Figure 6. Dependence of q_{in}/q_c on overpotential for Inconel 718.
$t_c = 20$ s.

14

Table 3
VALUES OF k_a AND J FOR INCONEL 718

Test	η (V)	E_c (V/SCE)	k_a (s^{-1})	J (nmol cm^{-2} s^{-1})
2	-0.10	-0.616	0.031	0.13
	-0.15	-0.671	0.035	0.15
	-0.20	-0.731	0.028	0.12
	-0.25	-0.790	0.035	0.08
3	-0.15	-0.628	0.031	0.23
	-0.20	-0.713	0.030	0.22
	-0.25	-0.783	0.030	0.15

INCOLOY 925

The values of k_a and J for four tests are given in Table 4. The low values of J imply that only a small amount of hydrogen entered the metal during t_c, and for this reason it was difficult to obtain precise values of q_a and therefore of k_a and J. Nevertheless, k_a does not appear to depend on overpotential and has a mean value of 0.006 ± 0.003 s^{-1}. Although the flux is small, it increases with overpotential. Values of q_a calculated using the derived values of k_a and J are compared with the corresponding experimental data ($\eta = -0.20$ V in test 10) in Figure 7, and again good agreement is observed over the range of charging times.

Data for q_T/q_{in} are shown in Figure 4. The charging current and therefore the charge (q_c) were low for the Incoloy, so it was not possible to determine reliable values of q_{in}/q_c. Unlike the Inconel, the Incoloy exhibits a linear dependence of q_T/q_{in} or $\sqrt{t_c}$ over the range of charging times studied, evidently as a result of its lower trapping constant .
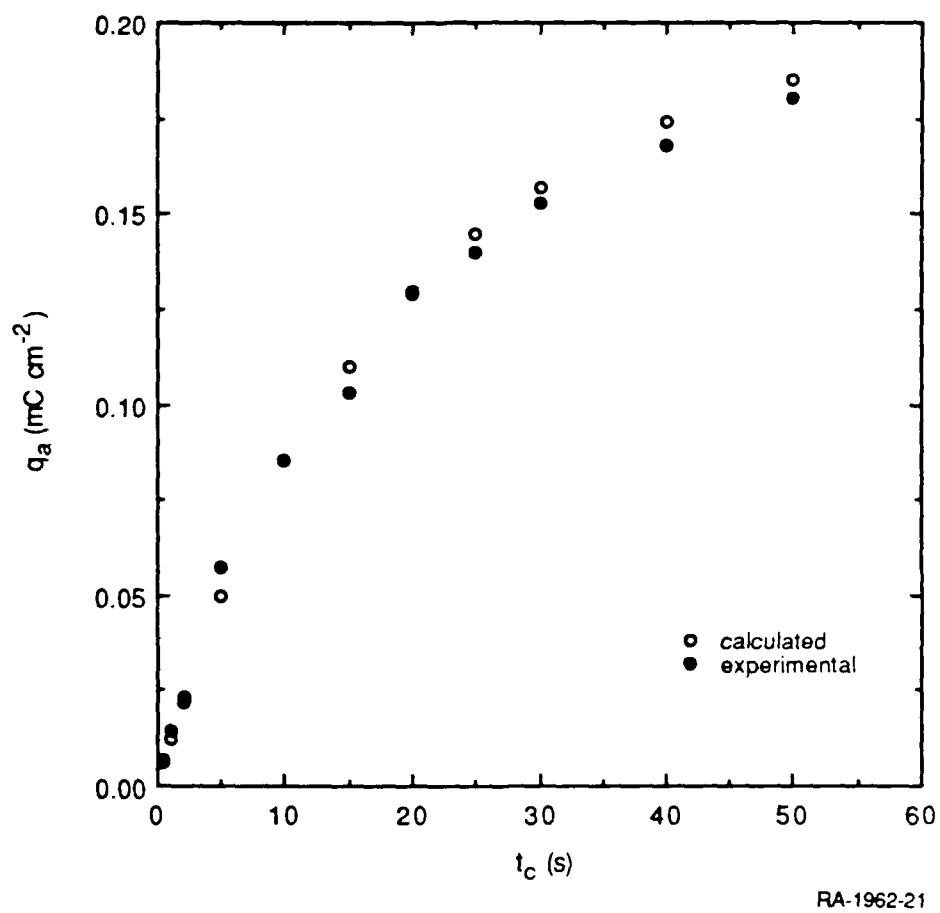
15

RA-1962-25

Figure 7. Comparison of experimental and calculated anodic charge
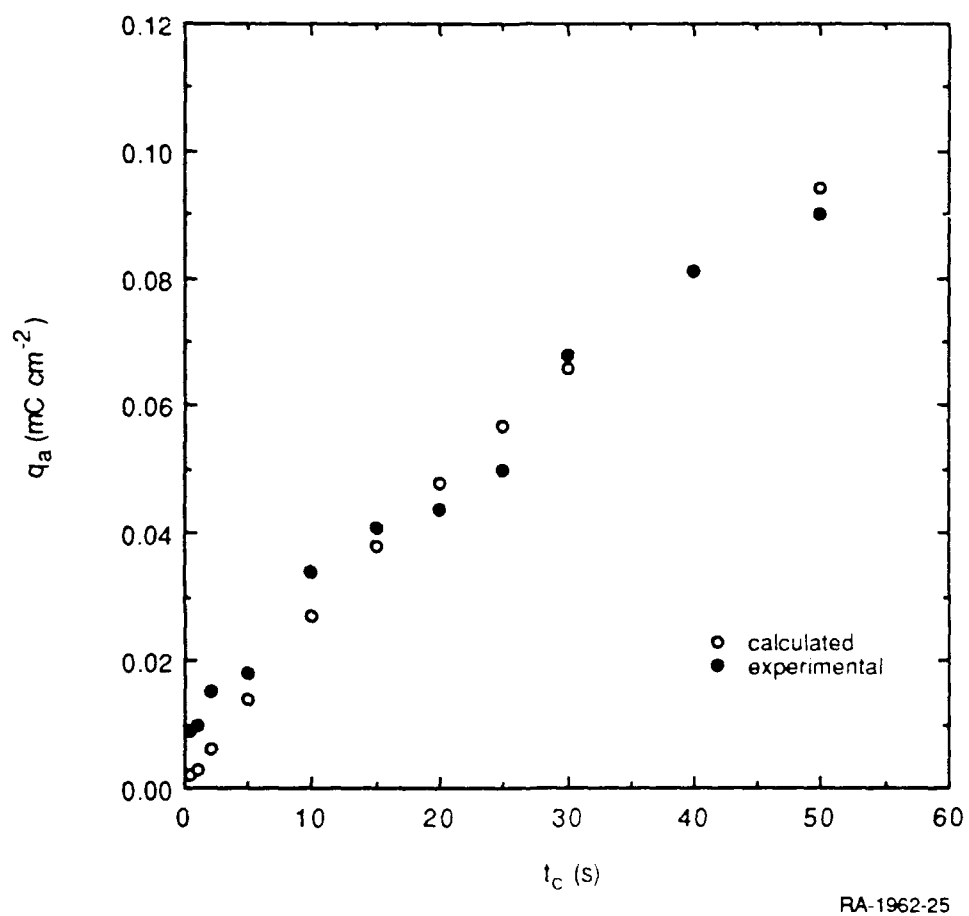data for Incoloy 925 in acetate buffer.

E_c = -0.369 V (SCE).

16

Table 4
VALUES OF k_a AND J FOR INCOLOY 925

Test	η (V)	E_c (V/SCE)	k_a (s^{-1})	J (nmol cm^{-2} s^{-1})
9	-0.25	-0.382	0.0013	0.02
	-0.30	-0.458	0.0088	0.05
10	-0.20	-0.369	0.0080	0.04
	-0.25	-0.414	0.0112	0.05
	-0.30	-0.476	0.0034	0.08
11	-0.25	-0.367	0.003	0.03
	-0.30	-0.427	0.006	0.06
12	-0.20	-0.383	0.005	0.02

18Ni MARAGING STEEL

The values of k_a and J for four tests are given in Table 5. The tests were performed in two pairs, with the two tests in a pair performed 1 hour apart and the two pairs separated by ~30 hours. The values of k_a for three of the tests (27, 28, and 30) are essentially independent of potential. In addition, the flux in these tests shows a small but systematic increase with overpotential. However, the trapping constants for test 27 are noticeably higher than those for test 28. Similarly, the k_a values for test 29 up to -0.2 V are higher than the corresponding values in test 30 but then decrease to values similar to those in tests 28 and 30.

The decrease in k_a suggests a filling of some traps, presumably to saturation level because k_a eventually becomes constant. In contrast, the change in k_a over 30 hours indicates that the traps are emptied over this period. This explanation implies that hydrogen diffusion in maraging steel is rapid enough to penetrate beyond the layer of metal removed during polishing before each test. The average diffusion distance (χ) can be estimated from Eq. (5).

$$\chi = (2Dt_c)^{1/2} \tag{5}$$

The maximum value of χ is 3.2 μm if it is assumed that $D = 1 \times 10^{-13}$ m^2 s^{-1} (see Discussion) and $t_c = 50$ s. On the basis of this value, it was concluded that polishing removed all the metal available to hydrogen via lattice diffusion and so exposed fresh traps. Therefore, residual

17

hydrogen must be related to deeper penetration of hydrogen by grain boundary diffusion. In the case of nickel, hydrogen diffusion along grain boundaries is known to be somewhat more rapid than through the lattice, but similar studies of maraging steel have apparently not been reported.

If residual hydrogen is assumed to be present, the change in trapping behavior can be explained by the effects of different types of traps. The apparent trapping constants for tests 27 and 29 probably reflect a combination of truely irreversible traps and quasi-irreversible traps (traps that are irreversible over minutes up to at least 1 hour but not for longer times spanning hours) whereas those for tests 28 and 30 are assumed to correspond to irreversible trapping only. In irreversible trapping, the rate constant for release is assumed to be zero, whereas for the quasi-irreversible case, the release constant is not zero but is too small achieve local equilibrium between the lattice and trapped hydrogen.

The densities of the irreversible and quasi-irreversible traps are assumed to be additive, so that in accordance with Eq. (4), k_a can be separated into two components:

$$k_a = k_a' + k_a''$$ (6)

where k_a' and k_a'' correspond to the irreversible and quasi-irreversible traps, respectively. The total trapping constant was determined as the mean of the results from test 27, giving $k_a = 0.015 \pm 0.003$ s^{-1}. The results for test 29 apparently reflect a transition from combined trapping to only irreversible trapping. The irreversible trapping constant was obtained as the mean of the results from tests 28 and 30, so that $k_a' = 0.005 \pm 0.002$ s^{-1}, and therefore $k_a'' = 0.010 \pm 0.005$ s^{-1}. Values of q_a calculated using k_a and J are compared with the corresponding experimental results ($\eta = -0.35$ V in test 28) in Figure 8, in which it is evident that the data are in close agreement over the full range of charging times.

Data for the charge ratios as a function of t_c are shown in Figures 4 and 9. As with the Incoloy, q_T/q_{in} for the maraging steel is linearly dependent on $\sqrt{t_c}$ over the range of interest. In addition, q_{in}/q_c exhibits a small linear dependence on t_c; as with the Inconel, this dependence lessens and eventually ceases with increasing overpotential. Also, as with the Inconel, q_{in}/q_c itself decreases with increasing overpotential (Figure 10), probably reflecting the relative increase in the rate of hydrogen recombination over hydrogen entry.
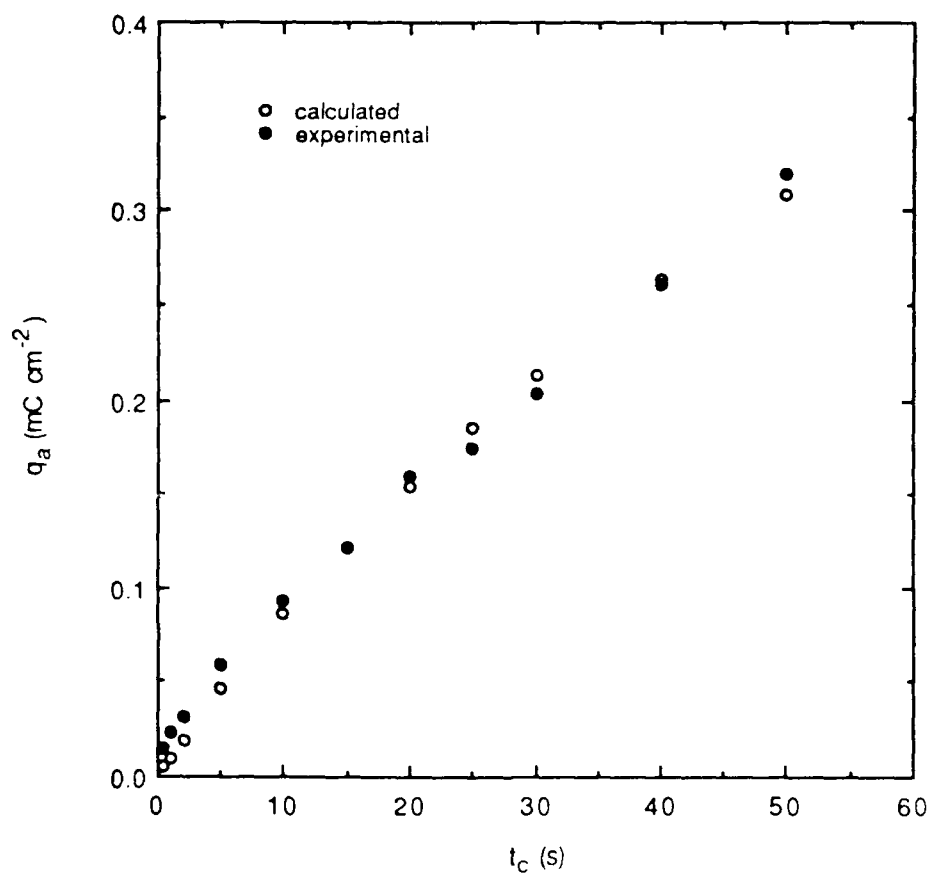
RA-1962-26

Figure 8. Comparison of experimental and calculated anodic charge
data for 18Ni maraging steel in acetate buffer.

E_c = -0.881 V (SCE)
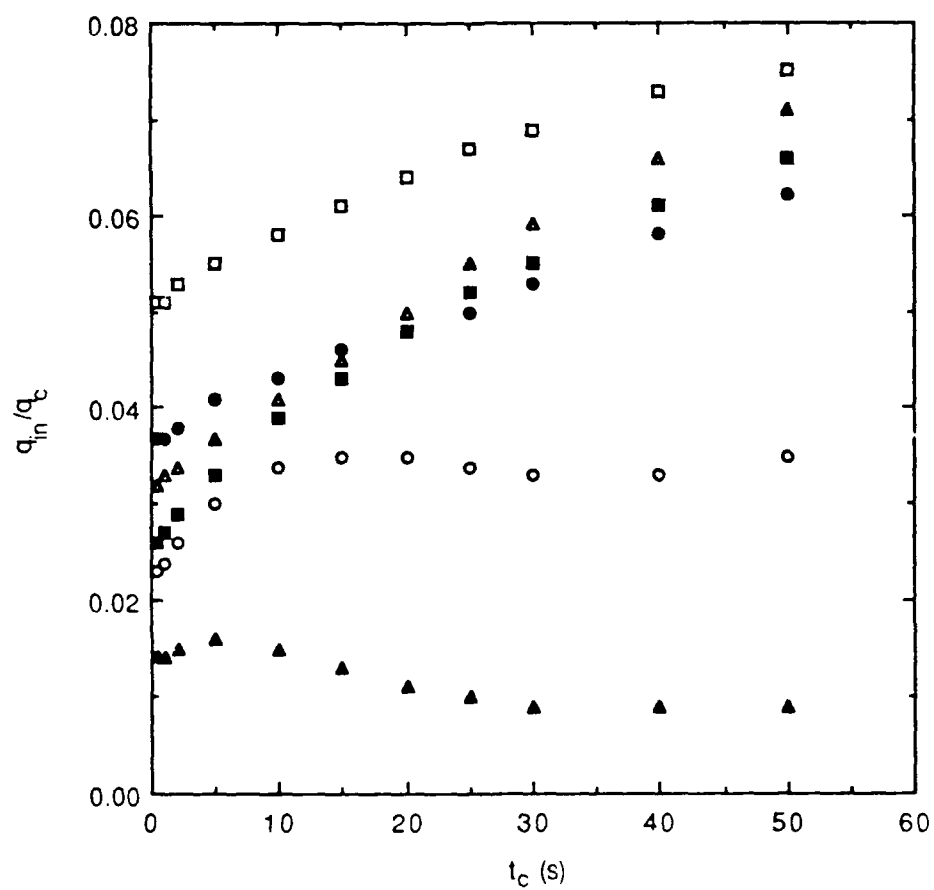
RA-1962-27

Figure 9. Dependence of q_{in}/q_c on charging time for 18Ni maraging
steel at various overpotentials.

□ -0.15 V; ● -0.20 V; ▲ -0.25 V; ■ -0.30 V;
○ -0.35 V; ▲ -0.40 V.

Figure 10. Dependence of q_{in}/q_c on overpotential for 18Ni maraging steel.

$t_c = 40$ s.

21

Table 5
VALUES OF k_a AND J FOR 18Ni MARAGING STEEL

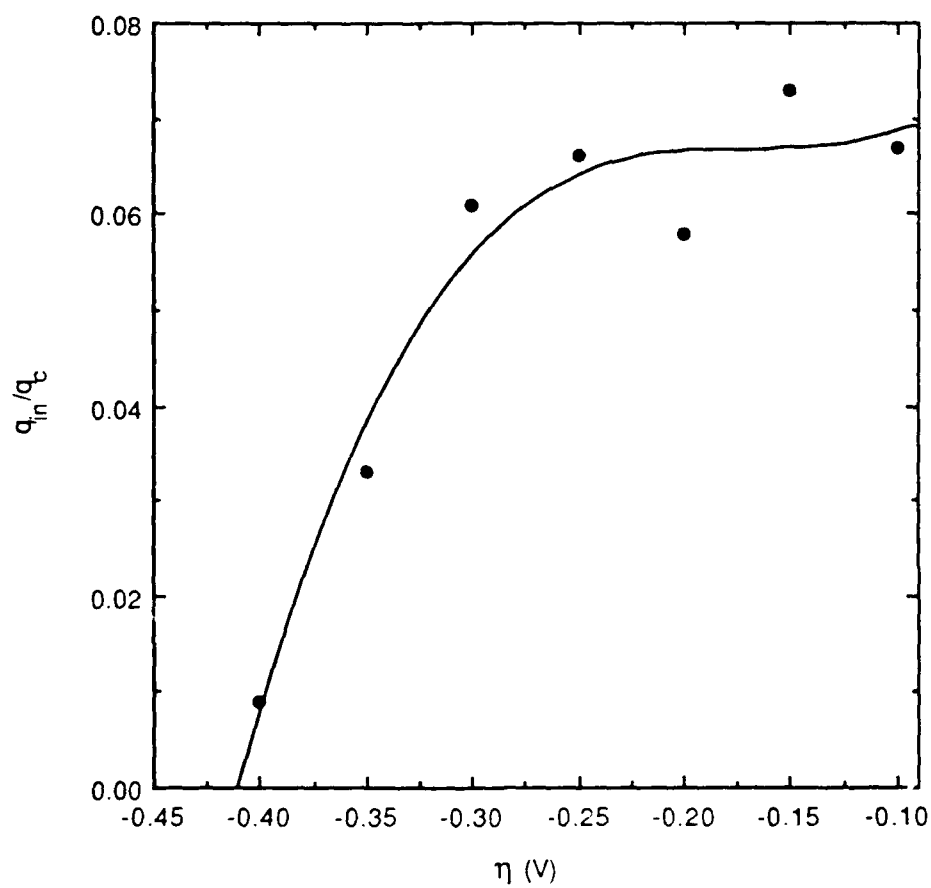| Test	η (V)	E_c (V/SCE)	k_a (s^{-1})	J (nmol cm^{-2} s^{-1})	Mean k_a
27	-0.10	-0.549	0.025	0.13	
	-0.15	-0.601	0.010	0.12	
	-0.20	-0.677	0.014	0.13	
	-0.25	-0.747	0.011	0.13	0.015 ± 0.003
	-0.30	-0.806	0.014	0.15	
	-0.35	-0.866	0.015	0.17	
	-0.40	-0.925	0.016	0.19	
28	-0.10	-0.600	0.003	0.04	
	-0.15	-0.655	0.007	0.06	
	-0.20	-0.710	0.003	0.07	
	-0.25	-0.768	0.004	0.08	0.006 ± 0.002
	-0.30	-0.826	0.006	0.09	
	-0.35	-0.881	0.007	0.11	
	-0.40	-0.940	0.010	0.14	
29	-0.10	-0.556	0.021	0.11	
	-0.15	-0.620	0.014	0.10	
	-0.20	-0.684	0.021	0.13	
	-0.25	-0.747	0.015	0.10	*
	-0.30	-0.806	0.007	0.09	
	-0.35	-0.863	0.004	0.10	
	-0.40	-0.919	0.008	0.12	
30	-0.10	-0.600	0.008	0.04	
	-0.15	-0.659	0.001	0.04	
	-0.20	-0.714	0.004	0.06	
	-0.25	-0.771	0.002	0.07	0.005 ± 0.002
	-0.30	-0.827	0.004	0.08	
	-0.35	-0.876	0.008	0.10	
	-0.40	-0.932	0.005	0.11	

* Mean not calculated because k_a changed at high overpotentials.

PURE TITANIUM

The anodic charge (q_a) was invariant with t_c, which is not predicted by the diffusion/trapping model for either diffusion or interface control. Therefore, k_a could not be determined at any potential over the wide range studied (-0.05 V to -0.8 V). The open-circuit potential, and therefore the charging potential, generally exhibited a positive shift over the range of charging times for each overpotential. This shift might compensate for the increase in t_c.

22

However, in several cases, E_c changed by ≤ 5 mV and q_a was essentially constant. Therefore, any effect resulting from the shift in E_c appears to be minor. Instead, the invariance in q_a indicates that negligible hydrogen enters the metal, so that q_{in} is approximately zero, and therefore q_a corresponds solely to oxidation of the adsorbed layer of hydrogen, that is, it should comprise only q_{ads}. The dependence of log q_a on η (Figure 11) is linear over a wide potential range, as expected if $q_a \sim q_{ads}$. The lack of dependence at high overpotentials probably corresponds to full coverage of the adsorbed hydrogen layer.
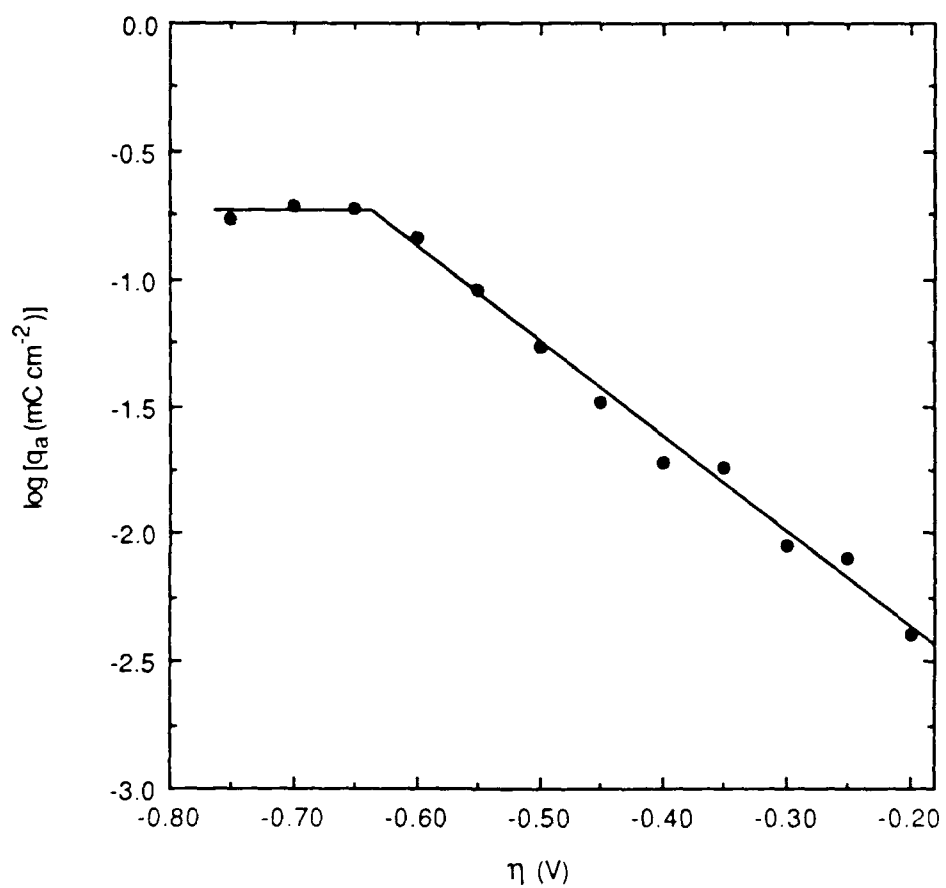
TITANIUM GRADE 2

Titanium grade 2, in contrast to the pure form, exhibits a marked dependence of q_a on t_c, so that trapping constants can be evaluated in this case. The values of k_a and J for two tests are given in Table 6. The flux increases with overpotential as a result of the dependence of J on the surface coverage of H_{ads}. The variation in log J with η shown in Figure 12 is linear, as is required with the assumption that the surface coverage responded rapidly to changes in potential.

In both tests, k_a is independent of overpotential but exhibits two values depending on the potential range. At charging potentials up to approximately -0.93 V, k_a is 0.028 ± 0.002 s^{-1}, whereas the mean value at higher potentials is 0.040 s^{-1}. Two further tests performed at high potentials gave trapping constants of 0.036 s^{-1} and 0.042 s^{-1}. The mean value of k_a at high potentials in the four tests was 0.040 ± 0.004 s^{-1}. Values of q_a calculated using k_a and J are compared with the corresponding experimental data ($\eta = -0.70$ V in test 23) in Figure 13, and again the data agree well over the charging time range.

The increase in trapping constant at high overpotentials can be ascribed to an additional type of irreversible trap participating concurrently with the irreversible traps detected at low overpotentials. The densities of the two traps are assumed to be additive, and therefore k_a at high overpotentials can be represented by

$$k_a = k_{a1} + k_{a2} \tag{7}$$

where k_{a1} corresponds to the irreversible traps detected at low η and k_{a2} is associated with the

23

RA-1962-29

Figure 11. Dependence of anodic charge on overpotential for pure titanium in acetate buffer.

24
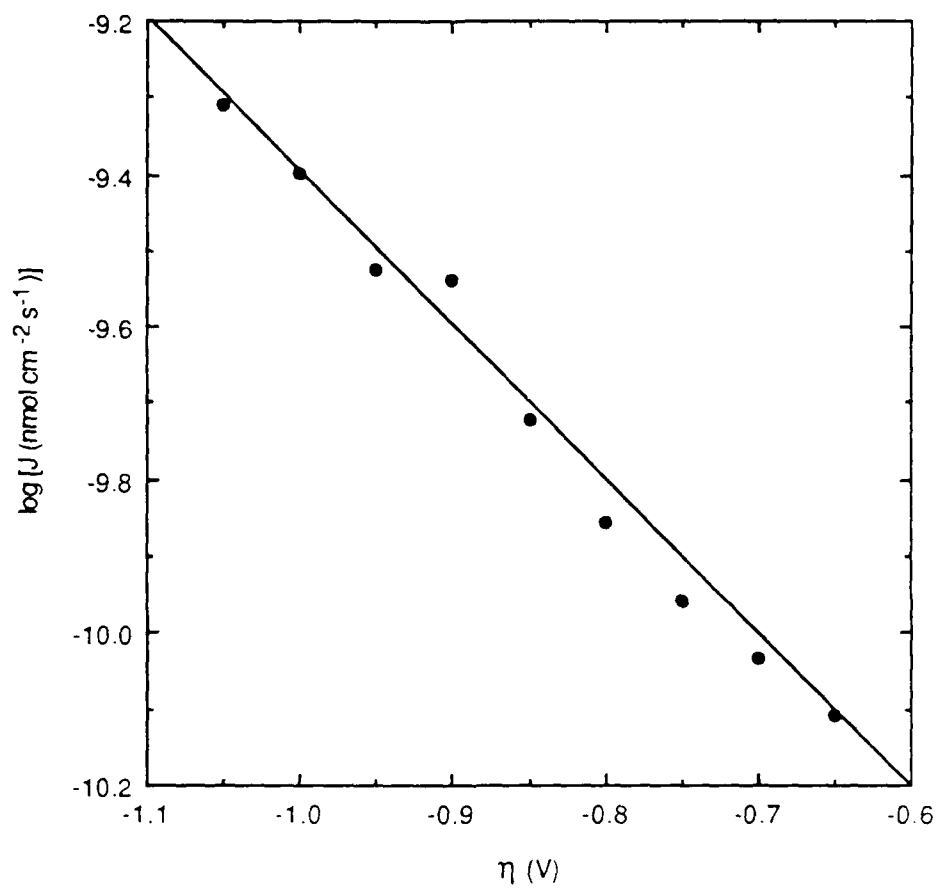
RA-1962-30

Figure 12. Dependence of flux on overpotential for titanium grade 2.

RA-1962-31

Figure 13. Comparison of experimental and calculated anodic charge
data for titanium grade 2 in acetate buffer.

$E_c = -0.741$ V (SCE).

26

additional type of trap. The total trapping constant (k_a) was taken as the mean (0.040 s^{-1}) of the high η results, and $k_{a1} = 0.028 \pm 0.002$ s^{-1}, so that $k_{a2} = 0.012 \pm 0.006$ s^{-1}.

Table 6
VALUES OF k_a AND J FOR TITANIUM GRADE 2

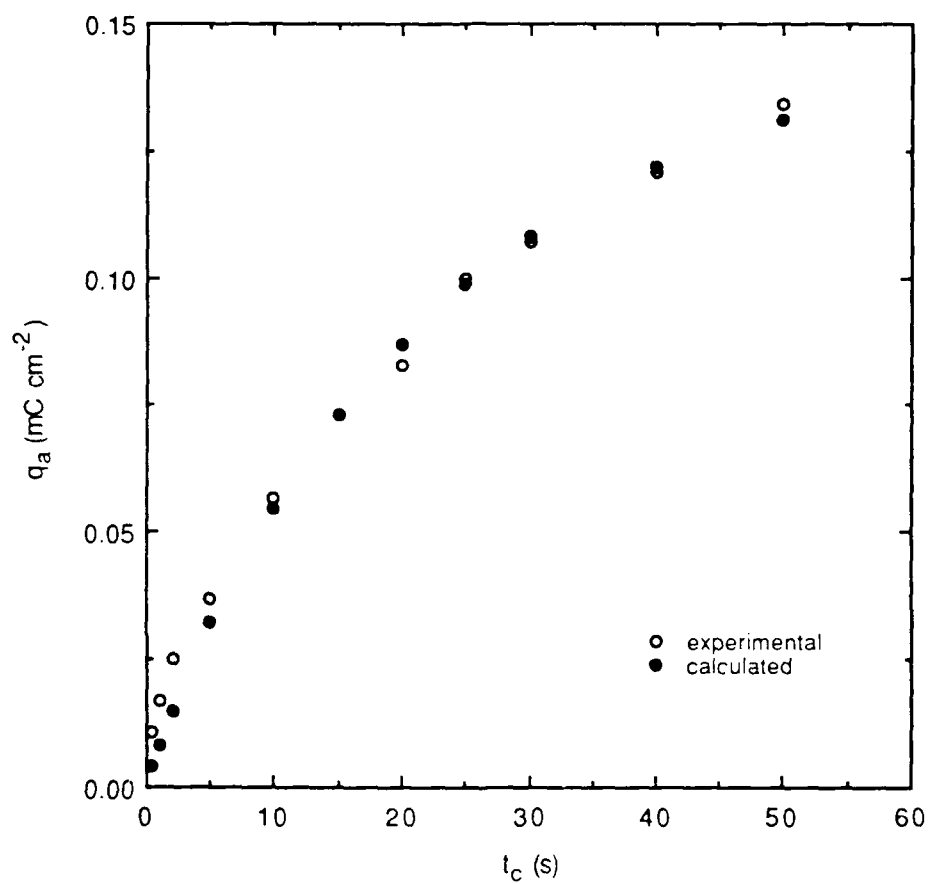| Test	η (V)	E_c (V/SCE)	k_a (s^{-1})	J (nmol cm^{-2} s^{-1})	Mean k_a
21	-0.55	-0.614	0.029	0.07	
	-0.60	-0.652	0.034	0.08	
	-0.65	-0.708	0.025	0.08	
	-0.70	-0.751	0.024	0.09	0.028 ± 0.002
	-0.75	-0.806	0.028	0.13	
	-0.80	-0.868	0.029	0.17	
	-0.85	-0.930	0.029	0.22	
	-0.90	-1.040	0.044	0.39	
	-0.95	-1.062	0.044	0.44	
	-1.00	-1.137	0.049	0.56	0.044 ± 0.002
	-1.05	-1.203	0.042	0.59	
	-1.10	-1.283	0.044	0.69	
	-1.15	-1.370	0.041	0.73	
23	-0.60	-0.655	0.031	0.07	
	-0.65	-0.692	0.028	0.08	
	-0.70	-0.741	0.029	0.09	0.028 ± 0.001
	-0.75	-0.796	0.027	0.11	
	-0.80	-0.857	0.027	0.14	
	-0.85	-0.921	0.028	0.19	
	-0.90	-0.987	0.034	0.29	
	-0.95	-1.024	0.033	0.30	
	-1.00	-1.111	0.039	0.40	0.036 ± 0.003
	-1.05	-1.182	0.041	0.49	
	-1.10	-1.258	0.035	0.49	
	-1.15	-1.310	0.034	0.51	

Data for the charge ratios as a function of t_c at low overpotentials are shown in Figures 4 and 14. As with the Inconel, q_T/q_{in} for titanium grade 2 shows some deviation from the empirical $\sqrt{t_c}$ dependence, which is likewise related to its relatively high trapping constant. The ratio of q_{in} to q_c
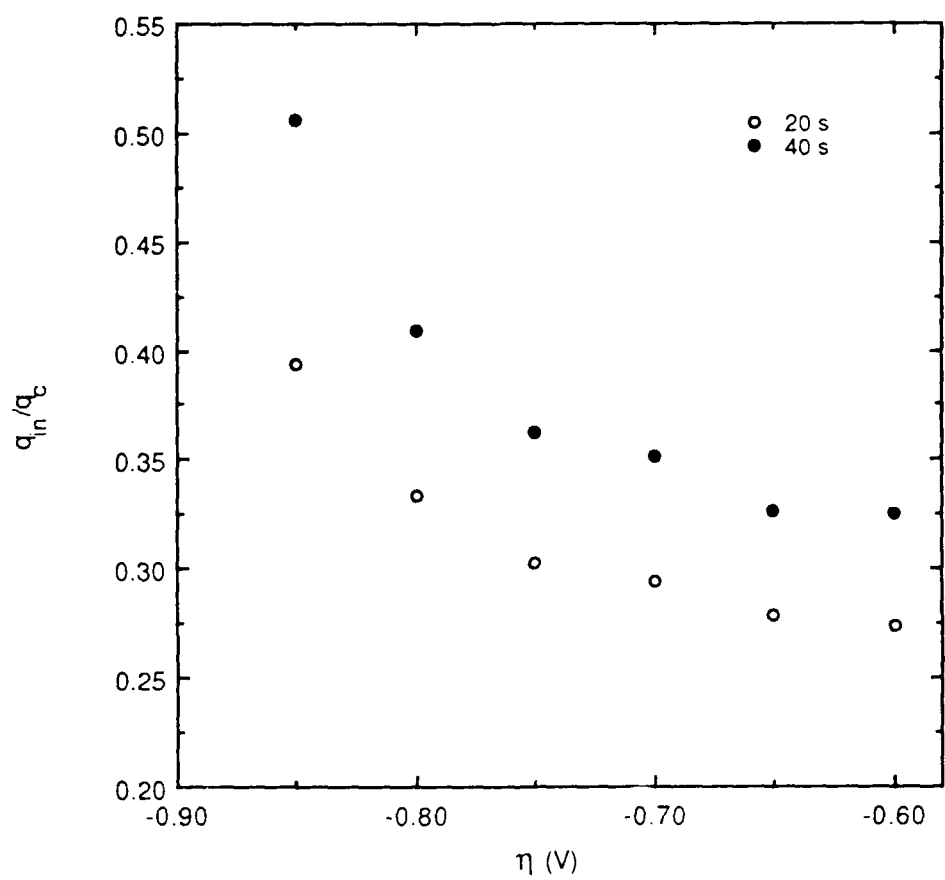
27
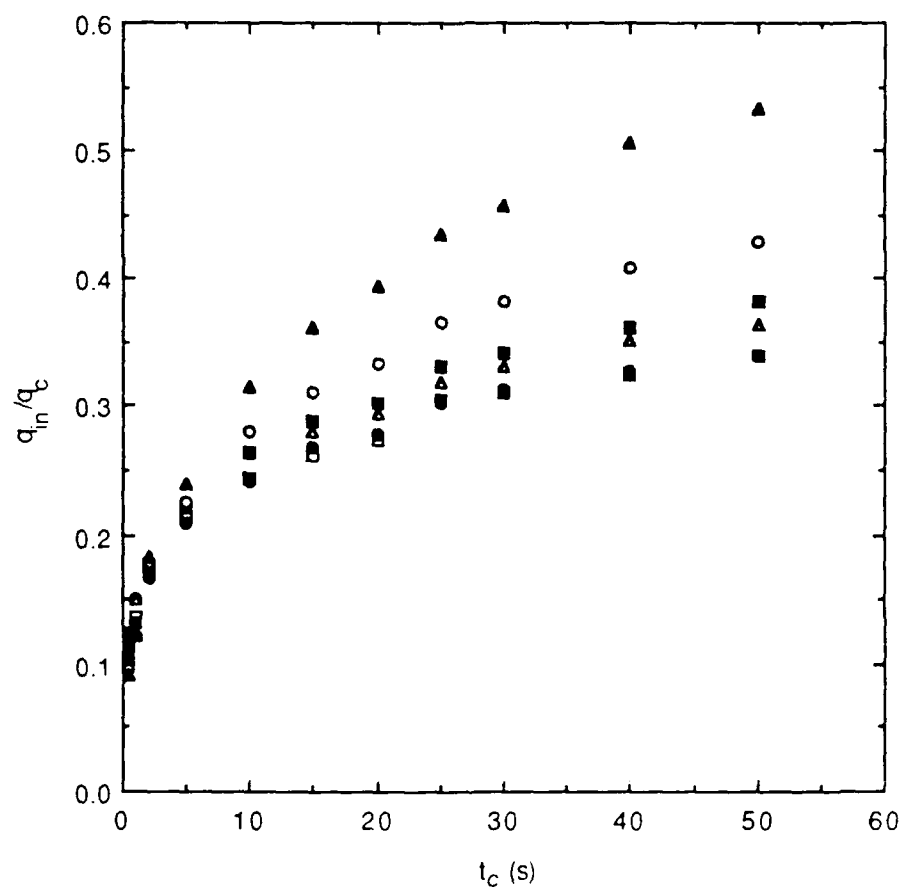
RA-1962-32

Figure 14. Dependence of q_{in}/q_c on charging time for titanium
grade 2 at low overpotentials.

□ -0.60 V; ● -0.65 V; ▲ -0.70 V; ■ -0.75 V;
○ -0.80 V; ▲ -0.85 V.

increases linearly with t_c. However, in contrast to that for the Inconel and maraging steel, this increase in q_{in}/q_c becomes greater at higher overpotentials (Figure 15). Since hydrogen entry becomes more efficient, hydrogen atom recombination during charging on Ti grade 2 must occur electrochemically, because chemical recombination should become more efficient than entry at high overpotentials. A similar result was obtained in studies[11] of titanium in sulfuric acid solutions between pH 0.25 and 2.25; under these conditions, hydrogen evolution is believed to occur on an oxide film at potentials more positive than approximately -1.0 V and to involve electrochemical desorption as the rate-determining step.

The data for q_T/q_{in} at high overpotentials exhibits similar non-linear behavior to that for this ratio at low overpotentials (Figure 4). In addition, q_{in}/q_c in general increases with t_c, as shown in Figure 16, but varies with η in the opposite manner from that found for low overpotentials; that is, q_{in}/q_c is high at the low end of the overpotential range and decreases as η increases (Figure 17). This reduction in the efficiency of hydrogen entry is presumably related to the higher trapping constant obtained for this overpotential range and can be explained by the formation of a hydride, as discussed later.

RA-1962-33

Figure 15. Dependence of q_{in}/q_c on overpotential for titanium grade 2 at low overpotentials and charging times of 20 s and 40 s.

30

RA-1962-34

Figure 16. Dependence of q_{in}/q_c on charging time for titanium
grade 2 at high overpotentials

□ -0.90 V; ● -0.95 V; ▲ -1.00 V; ■ -1.05 V ;
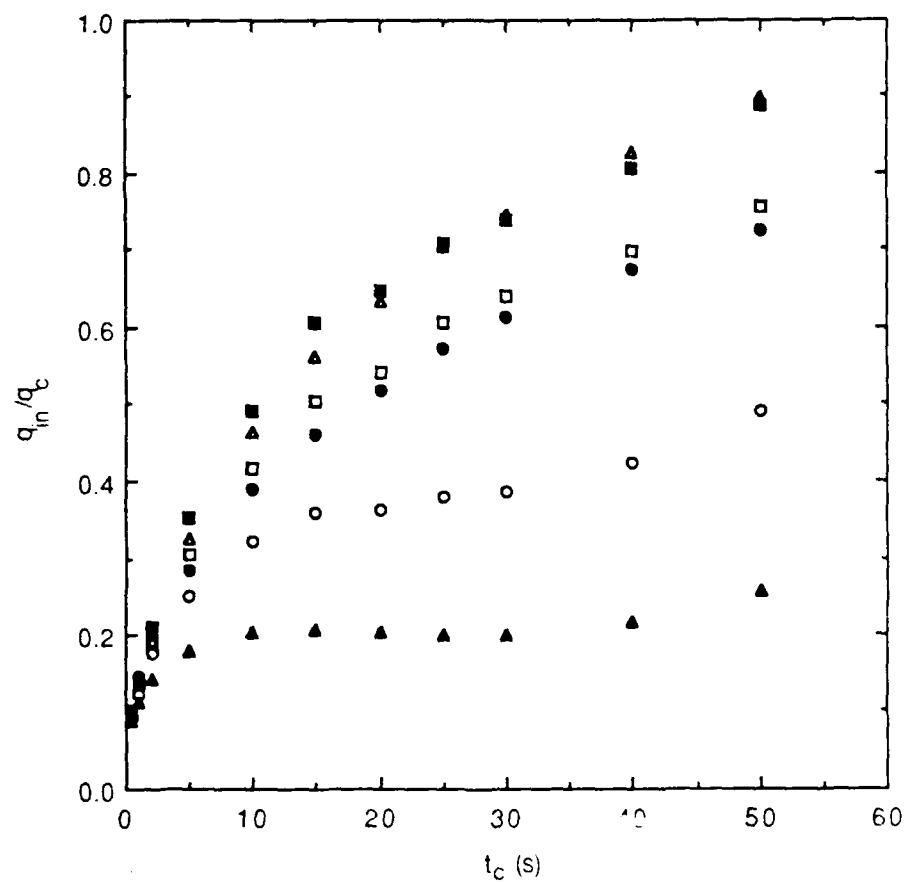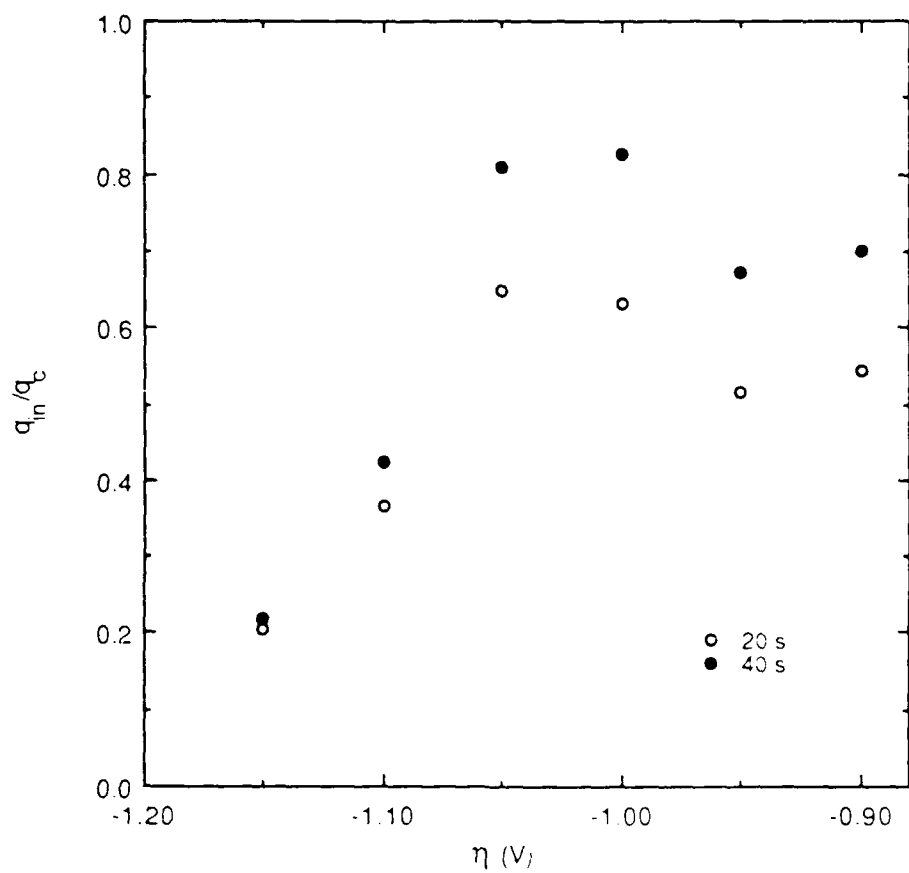○ -1.10 V; ▲ -1.15 V.

31

RA-1962-65

Figure 17. Dependence of q_{in}/q_c on overpotential for titanium grade 2 at high overpotentials and charging times of 20 s and 40 s.

32

DISCUSSION

INCONEL 718

Irreversible Trapping Constant

The irreversible trapping constant (k) can be obtained from k_a by using diffusivity data for the pure Fe-Ni-Cr alloy to obtain D_L and for Inconel 718 to obtain D_a. The minor alloying elements are assumed to be primarily responsible for the reversible trapping behavior in the Inconel because the binding energy of hydrogen to defects such as vacancies or edge dislocations in an fcc lattice is a factor of four smaller than the activation energy for diffusion. The apparent diffusivity for hydrogen in Inconel 718 has been measured as a function of temperature from $150°$ to $500°C$ and is given (in $m^2 s^{-1}$) by the following equation:[12]

$$D = 1.07 \times 10^{-6} \exp [(-49790 \text{ J mol}^{-1})/RT] \tag{8}$$

Extrapolation to 25°C gives a value of 2.0×10^{-15} $m^2 s^{-1}$, which is consistent with the diffusivities of other nickel-base alloys at ambient temperature. The most appropriate diffusivity data[13] for the pure Ni-Cr-Fe alloy are for 76% Ni-16% Cr-8% Fe, for which D_L is $(7.9 \pm 1) \times 10^{-15}$ $m^2 s^{-1}$. Although the levels of the three elements, especially Ni and Fe, differ to some extent in the pure alloy and the Inconel, the error in using the diffusivity of the Ni-Cr-Fe alloy for D_L is assumed to be small enough to ignore. Accordingly, by using these data for D_L and D_a, K_r is found to be 3.0 $\pm$ 0.5 and, therefore, the value of k is 0.124 ± 0.024 s^{-1}.

Identification of Traps

Previous studies have shown that carbide-matrix interfaces are irreversible traps.[3,14,15] The trapping energy for hydrogen at Fe_3C and TiC interfaces is 77-87 kJ mol^{-1}, which is well in excess of the value of 58 kJ mol^{-1} considered to delineate irreversible and reversible trapping.[3,16] Accordingly, the irreversible traps in Inconel 718 are assumed to be the niobium carbide particles.

The density of the irreversible trap particles was calculated from the trapping constant by using Eq. (4). The diameter (a) of the metal atom was taken as the mean of the atomic diameters of Fe (248 pm), Ni (250 pm), Cr (250 pm), and Mo (272 pm) weighted in accordance with the atomic fraction of each element in the alloy. The assumption of a spherical shape is clearly an approximation for carbide particles in the Inconel. However, by using the value of 3.9 μm for the

mean radius of the carbide particles, $D_a = 2.0 \times 10^{-15}$ m^2 s^{-1}, and a $= 250 \times 10^{-12}$ m, the density of trap particles was calculated to be 2.0×10^{13} m^{-3}. The agreement between the actual concentration of carbide particles (2.2×10^{13} m^{-3}) and the trap density is remarkable in view of the assumed spherical shape for the traps and carbides. This close agreement does indicate clearly that large traps with both a high surface area and a high trapping energy can overwhelmingly dominate the irreversible trapping behavior of an alloy.

INCOLOY 925

Irreversible Trapping Constant

Evaluation of the irreversible trapping constant (k) from k_a requires diffusivity data for the pure Fe-Ni-Cr alloy to obtain D_L and for Incoloy 925 to obtain D_a. As with Inconel 718, the minor alloying elements are assumed to be primarily responsible for the reversible trapping behavior in the Incoloy. Data do not appear to be available for Incoloy 925, but the apparent diffusivity for hydrogen in Incoloy 903 over the temperature range 150° to 500°C is given (in m^2 s^{-1}) by the following equation[12]:

$$D = 2.46 \times 10^{-6} \exp [(-52677 \text{ J mol}^{-1})/RT] \qquad (9)$$

Extrapolation to 25°C gives a value of 1.4×10^{-15} m^2 s^{-1}. The most appropriate diffusivity data for the pure alloy are those for the 76% Ni-16% Cr-8% Fe (see Inconel 718 above). The difference in the levels of the three elements between the pure alloy and the Incoloy is larger than that in the case of the Inconel but, in the absence of more appropriate data, the error in using the diffusivity of the Ni-Cr-Fe alloy for D_L still has to be treated as negligible. These data for D_L and D_a were used to obtain a value of 4.6 ± 0.6 for K_r, and so k was found to be 0.034 ± 0.004 s^{-1}.

Identification of Traps

Hydrogen-induced fracture in Incoloy 903 is initiated by void formation at matrix carbides.[17] Accordingly, the TiC particles were assumed to provide the irreversible traps in Incoloy 925. The trapping constant for this alloy was used to calculate the density of irreversible trap particles by means of Eq. (4). The diameter (a) of the metal atom in the Incoloy was taken as the weighted mean of the atomic diameters of Fe, Ni, Cr, Mo, and Ti (290 pm). Although the spherical trap shape assumed in deriving Eq. (4) is again somewhat of an approximation for carbide particles in the Incoloy, the carbide particles were assumed to have a mean radius of 1.4

μm. By using $D_a = 2.0 \times 10^{-15}$ m^2 s^{-1} and a = 250 x 10^{-12} m, the density of trap particles was calculated to be 4.1 x 10^{13} m^{-3}. The actual concentration of carbide particles (4.6 x 10^{13} m^{-3}) and the trap density are again in close agreement despite the assumption that the traps and carbides are spherical.

18Ni MARAGING STEEL

Irreversible Trapping Constant

The mechanical properties and hydrogen permeation parameters for 18Ni (250) maraging steel have been studied as a function of aging temperature.[18] The diffusivity of hydrogen was found to decrease as the aging temperature increases, whereas the hardness increases up to a maximum of about HRC 52 at 500°C and then decreases. The diffusivity for the 18Ni (250) steel aged at 480°C is approximately 3.7 x 10^{-13} m^2 s^{-1}. A comparison[9] with other results indicates that the room temperature diffusivity for hydrogen in maraging steels is between 10^{-12} and 10^{-13} m^2 s^{-1}. The 250-ksi grade of 18Ni maraging steel nominally contains a little over half as much titanium as does the 300-ksi grade, and previous work has shown that the diffusivity of hydrogen in iron is inversely proportional to the titanium content.[9] Therefore, the diffusivity for the 18Ni (300) steel used in this study is assumed to be 1 x 10^{-13} m^2 s^{-1}, allowing for the higher hardness (HRC 53.8) of this grade.

Diffusivity data for the pure Fe-Ni-Co-Mo alloy do not appear to be available. The most appropriate data are those for Fe-Ni alloys,[19] for which D_L (18% Ni) is ~3 x 10^{-11} m^2 s^{-1} at 27°C. It has been suggested on the basis of previous studies that the difference in diffusivity between Fe-20% Ni and pure iron may be related to trapping effects of the martensitic structure.[9] Accordingly, minor elements, especially Co and Mo, are assumed to have little effect on the diffusivity in the Fe-Ni-Co-Mo alloy. By using the appropriate data for D_L and D_a, K_r was calculated to be 300 ± 90, and therefore k' = 1.50 ± 1.05 s^{-1} and k"= 3.0 ± 2.4 s^{-1}.

Identification of Traps

Quasi-irreversible Traps. The change in k_a between experiments performed 30 hours apart indicates that hydrogen remaining desorbs slowly, which in turn suggests the formation of an unstable hydride during charging. This possibility is consistent with the behavior of Hastelloy C-276, which is known to form an unstable hydride that slowly dissociates over 20 hours at room temperature.[20] Moreover, the C-276 appears to form an alloy hydride rather than NiH.

Potential traps are the intermetallic compounds, Ni_3Mo and possibly Ni_3Ti or FeTi, precipitated during age hardening of the maraging steel.[21] The energy of hydrogen interaction with the intermetallic particles has been estimated to be 38.6 kJ mol⁻¹.[22] This value was derived by assuming equilibrium between the traps and lattice but is reasonable when compared with the interaction energies of other metallic traps.[23] The interaction energy for the intermetallics suggests that they are reversible traps, which is perhaps to be expected because reversibility was assumed in the calculation. Nevertheless, these intermetallics have to be considered as possibilities for the trap sites from which slow release of hydrogen occurs. In addition, the submicroscopic size of the intermetallics would make them likely to be filled during the charging time used in the pulse tests.

The size of the precipitate particles is generally several hundred Angstroms in their largest dimension, and the interparticle spacings are on the order of 300 to 500 Å.[21] The trap density calculated using these values was 2×10^{16} m⁻³, which is about 5 orders of magnitude lower than the estimated concentration of intermetallic particles. Therefore, the principal quasi-irreversible trap is evidently not a primary or secondary intermetallic precipitate. Rather, these precipitates would appear to be reversible traps, as is implied by the magnitude of their interaction energy.

Another possibility is that the quasi-irreversible trap is associated with microstructural boundaries. Autoradiography studies using tritium have shown that trapping occurs at grain boundaries and martensite boundaries in maraging steel.[24,25] In addition, the location of tritium in the alloy is virtually unchanged after two months except for a small amount of outgassing. Therefore, both sites appear to be moderately strong traps in maraging steel, although grain boundaries are generally considered to be reversible traps in ferritic steels. It is possible that the martensite boundaries are stronger traps than the grain boundaries and so tend more toward irreversibility. If the martensite boundaries as well as the grain boundaries are assumed to have an influence diameter of 3 nm,[23] the trap density is found to be 9×10^{17} m⁻³.

At this stage, the quasi-irreversible trap remains unidentified. A quasi-reversible trap should have a trapping energy close to the value (58 kJ mol⁻¹) representing the boundary between reversible and irreversible trapping. However, none of the elements in the maraging steel appear to fulfil this requirement. In fact, the trapping energies for most of the atomic traps are well below the range of values for the interfaces and can be treated as reversible.[16,23] Moreover, the density of traps determined from k" by assuming one of the possible atomic traps such as Zr is about 5 to 6 orders of magnitude lower than the actual number of atoms calculated from the composition of the alloy.

36

Irreversible Traps. Intense hydrogen trapping has been observed at carbo-nitride interfaces in maraging steels by using autoradiography[24,25] and indicates Ti(CN) as an irreversible trap in these steels. Accordingly, the density of irreversible traps was calculated using Eq. (4) based on Ti(CN) particles. The diameter (a) of the metal atom was taken as the weighted mean of the atomic diameters of Fe, Ni, Mo, Ti, and Co (250 pm). The carbide particles were again treated as spherical, and the trap radius was taken as 1.7 μm. By using $D_a = 2.0 \times 10^{-15}$ m^2 s^{-1} and a = 250 x 10^{-12} m, the density of traps was calculated to be 3.4×10^{11} m^{-3}, as compared with $(1.1 \pm 0.6) \times 10^{13}$ m^{-3} for the actual concentration of carbide particles. The two values differ by a factor of ~30, which can be accounted for to a large extent, if not entirely, by the uncertainties in both the concentration of particles and the value of D_a assumed for the 300-ksi grade of 18Ni maraging steel. In view of these uncertainties, the calculated trap density and carbide concentration are considered to correlate moderately well.

PURE TITANIUM

Titanium in the pure form appears to be resistant to hydrogen penetration. The surface film formed on pure titanium in aqueous solutions is known to be a highly effective barrier to hydrogen entry. Thus, the anodic charge data are consistent with the presence of a hydrogen barrier. Previous work on single crystal TiO$_2$ in the rutile form[26] has shown that the diffusivity of hydrogen at 20°C is about 4 orders of magnitude higher for the c-axis (1.9×10^{-16} m^2 s^{-1}) than for the a-axis (7.5×10^{-20} m^2 s^{-1}). Therefore, the film orientation can largely determine the resistance of titanium to hydrogen entry, which may account for the difference in charging behavior of the pure and grade 2 forms of titanium.

TITANIUM GRADE 2

Irreversible Trapping Constant

The irreversible trapping constants (k_1 and k_2) for Ti grade 2 can be approximated to the apparent trapping constants on the basis of the low diffusivity of hydrogen in titanium and the closeness in the composition of the grade 2 metal and pure titanium. The diffusivity of hydrogen in α-Ti over the temperature range 25°-100°C is expressed by

$$D = 6 \times 10^{-6} \exp [(-60250 \pm 3347 \text{ J mol}^{-1})/RT] \text{ m}^2 \text{ s}^{-1} \qquad (10)$$

which gives a value of 1.65×10^{-16} m^2 s^{-1} at 25°C.[27] Because of the diffusivity and composition factors, the diffusivities for the pure and commercial grades are assumed to differ negligibly, so that $D_a \sim D_L$, and therefore $k = k_a$. Hence, $k_1 = 0.028 \pm 0.002$ s^{-1} and $k_2 = 0.012 \pm 0.006$ s^{-1}.

Identification of Traps

The trapping at low overpotentials as reflected by the value of 0.028 s^{-1} for k_1 could be associated with either the minor elements (C, N, O, and Fe) or structural defects such as grain boundaries and dislocations in the titanium. The density of irreversible traps was calculated from k_1 by assuming that the individual elements were the principal type of trap. The diameter (a) of the titanium atom was taken as 290 pm. The values of N_i and the atomic concentration (A) of the elements are given in Table 7.

Table 7
VALUES OF N_i FOR TITANIUM GRADE 2

Element	d (pm)	N_i (m^{-3})	A (m^{-3})	A/N_i
C	77	6.8×10^{23}	4.8×10^{25}	71
N	74	7.4×10^{23}	1.4×10^{25}	19
O	74	7.4×10^{23}	2.7×10^{26}	365
Fe	124	2.6×10^{23}	8.3×10^{25}	316

The ratio A/N_i represents the level of agreement between the atomic concentration and the trap density calculated on the basis of the appropriate element. In all cases except nitrogen, A/N_i is large enough to discount these elements as the principal irreversible trap, even allowing for the uncertainty in the hydrogen diffusivity which could vary N_i by a factor of almost 4. Moreover, oxygen is known to reduce the solubility of hydrogen in titanium,[26] which suggests that oxygen is unlikely to be a potential trap; this is consistent with the above results. However, a reasonable correlation exists for nitrogen, particularly because the uncertainty factor means that the calculated trap density may be no more than five times larger than the actual concentration of nitrogen atoms. Interestingly, among the interstitials, nitrogen is particularly effective in reducing the ductility of titanium,[28] which coincides with its apparent role as the principal irreversible trap. Hence, nitrogen may strongly affect the susceptibility of grade 2 titanium to hydrogen embrittlement

38

through its combined influence on brittleness and hydrogen trapping.

Although the data suggest that the principal irreversible trap may be nitrogen, grain boundaries are another possibility but, in the case of steels, the trapping energy of grain boundaries and therefore their reversible/irreversible nature depend on their angular orientation.[23] A more likely alternative is that trapping results from hydride formation. Hydride decomposition is expected to be slow relative to the duration of a pulse test, and hence the hydrogen can be considered irreversibly trapped.

Previous work has shown that unalloyed titanium absorbs hydrogen in near-neutral brine at 25° and 100°C when the potential is more negative than -0.75 V (SCE).[29] Only thin surface hydride films were found to form at potentials more positive than -1.0 V (SCE), but extensive hydride formation may occur at more negative potentials. Traps corresponding to the formation of a surface hydride could be expected to saturate at potentials approaching the commencement of accelerated hydride formation because of the decreasing availability of free titanium in the vicinity of the surface. Trap saturation would lead to a decrease in k_1 with increasing overpotential, but such a decrease is not observed. Therefore, it seems more likely that nitrogen rather than surface hydride formation or grain boundaries acts as the principal trap at low overpotentials. The additional trapping constant (k_2) obtained at high overpotentials [$E_c < -0.93$ V(SCE)] is probably associated with the accelerated formation of hydrides. Moreover, the decrease in q_{ir}/q_c in this potential region is consistent with the presence of a partial barrier to hydrogen entry and provides support for the formation of a thick hydride layer.

COMPARISON OF TRAPPING PARAMETERS

The mean values of the trapping constants for the three nickel-containing alloys and titanium grade 2 are summarized in Table 8. The maraging steel has the highest value of the irreversible trapping constant, followed by the Inconel and then the Incoloy and Ti grade 2. The high trapping constant for the steel compared with that for the Inconel is consistent with their relative susceptibilities to hydrogen embrittlement. Previous work on 18Ni (250) maraging steel and Inconel 718 subjected to stress-rupture tests during electrolytic charging has shown that the steel undergoes severe embrittlement, whereas the Inconel exhibits negligible susceptibility.[30,31]

39

Table 8
TRAPPING PARAMETERS

Alloy	k_a (s^{-1})	K_r	k (s^{-1})
Inconel 718	0.031 ± 0.002	3.0 ± 0.5	0.128 ± 0.024
Incoloy 925	0.006 ± 0.003	4.6 ± 0.6	0.034 ± 0.004
Maraging steel	0.005 ± 0.002 $0.010 \pm 0.005^*$	300 ± 90 300 ± 90	1.50 ± 1.05 $3.00 \pm 2.40^*$
Ti grade 2	0.028 ± 0.002 $0.012 \pm 0.006^\dagger$	n n	0.028 ± 0.002 0.012 ± 0.006

* Quasi-irreversible trapping
† Hydride formation
n = Not available

No Incoloys were included in the electrolytic charging tests, but gas phase charging studies on Incoloy 903 have shown that brief exposure to high pressure hydrogen is not detrimental although prolonged exposure, particularly at higher temperatures, can accumulate enough internal hydrogen to reduce ductility.[32] In contrast, gas phase charging of Inconel 718 causes embrittlement characterized as extreme.[30] These results suggest that Incoloy 903 and, by implication, Incoloy 925 are less sensitive than Inconel 718 to hydrogen embrittlement, so the order of the trapping constants for Inconel 718 and Incoloy 925 evidently parallels their relative susceptibilities to hydrogen embrittlement.

From the trapping constants for the nickel-containing alloys, the susceptibility of Ti grade 2 to hydrogen embrittlement at low levels of hydrogen is predicted to be similar to that of the Incoloy. Although hydride precipitates can be observed in grade 2 titanium at hydrogen concentrations above ~100 ppm, they do not cause gross embrittlement of the titanium until hydrogen levels exceed 500-600 ppm.[33] Therefore, the similarity in trapping constants for the Incoloy and titanium fits their relative resistance to hydrogen embrittlement in that long exposure times are required for the concentration of hydrogen to exceed the level necessary to result in a loss of mechanical properties. Furthermore, the higher trapping constant (0.040 s^{-1}) associated with the occurrence of significant hydride formation coincides with the increasing susceptibility to embrittlement with hydrogen concentration.

Finally, the irreversible trapping constants for the three nickel alloys and titanium provide an interesting comparison with those obtained earlier[6] for 4340 steel, Monel K-500 (nominally 65Ni-35Cu), and MP35N (nominally 35Ni-35Co-20Cr-10Mo). The values of k for the full range of alloys are listed in Table 9 in descending order. Clearly, there is a strong correlation between the hydrogen embrittlement susceptibility and the trapping capability of the alloy as represented by the irreversible trapping constant. The trapping constants for the three alloys studied earlier fit the overall trend in susceptibility and, as might be expected, indicate that the 4340 steel is the most susceptible followed by the maraging steel, which has a somewhat lower sensitivity on the basis of its value of k. At the other extreme, the low trapping constant for MP35N is consistent with the high resistance to hydrogen embrittlement found in practice for this alloy.[34,35]

Table 9
IRREVERSIBLE TRAPPING CONSTANTS

Alloy	k (s^{-1})
4340 steel	4
18Ni (300) maraging steel	1.5-3.0
Inconel 718	0.128
Monel K-500	0.040
Ti grade 2 (high H)	0.040
Incoloy 925	0.034
Ti grade 2 (low H)	0.028
MP35N	0.027

SUMMARY

- The ingress of hydrogen in three precipitation-hardened alloys (Inconel 718, Incoloy 925, and 18Ni maraging steel) and titanium grade 2 was shown to fit a diffusion/trapping model under interface control. Pure titanium does not absorb hydrogen because of the effectiveness of the surface oxide as a barrier to entry.

- The Inconel 718 and Incoloy 925 are each characterized by a single type of irreversible trap. The calculated trap densities indicated that these traps are NbC and TiC particles, respectively. In contrast, the maraging steel is characterized both by an unidentified quasi-irreversible trap and an irreversible trap thought to be TiC particles.

- In the case of titanium grade 2, interstitial nitrogen appears to be the principal irreversible trap at low hydrogen levels, although grain boundaries are another possibility. When the concentration of hydrogen becomes high enough, hydride formation provides an additional form of trapping.

- The irreversible trapping constants for the three nickel-containing alloys and Ti grade 2 are consistent with their relative susceptibilities to hydrogen embrittlement, with the maraging steel having the highest value, followed by the Inconel and then the Incoloy and Ti grade 2. Moreover, a comparison with 4340 steel and two other nickel-base alloys (Monel K-500 and MP35N) indicates that a strong correlation exists between hydrogen embrittlement susceptibility and trapping capability over the full range of these alloys.

- The diffusion/trapping model allows a range of microstructural features associated with carbides, hydride formation, and interstitial elements or grain boundaries to be identified as the predominant irreversible traps, either singly or in the presence of multiple principal traps. Moreover, the trapping capability of the individual alloys can be compared to provide a basis for explaining differences in the susceptibility of these alloys to hydrogen embrittlement.

REFERENCES

1. R. Gibala and D. S. DeMiglio, in *Proceedings of the 3rd International Conference on the Effect of Hydrogen on the Behavior of Materials*, I. M. Bernstein and A. W. Thompson, Eds. (The Metallurgical Society of AIME, Moran, Wyoming, 1980), p. 113.

2. G. M. Pressouyre and I. M. Bernstein, Metall. Trans. **9A**, 1571 (1978).

3. G. M. Pressouyre and I. M. Bernstein, Acta Metall. **27**, 89 (1979).

4. R. McKibbin, D. A. Harrington, B. G. Pound, R. M. Sharp, and G. A. Wright, Acta Metall. **35**, 253 (1987).

5. B. G. Pound. R. M. Sharp, and G. A. Wright, Acta Met. **35**, 263 (1987).

6. B. G. Pound, Corrosion **45**, 18 (1989); **46** (in press, 1990).

7. H. L. Eiselstein, "Advances in the Technology of Stainless Steels and Related Alloys," Special Technical Publication No. 369, ASTM (1965).

8. G. F. Vander Voort and H. M. James, in *Metals Handbook*, 9th ed., Vol. 9 (ASM, Metals Park, Ohio, 1987), p. 316.

9. D. P. Dautovich and S. Floreen, in *Proceedings of the Conference on the Stress Corrosion Cracking and Hydrogen Embrittlement of Iron-Base Alloys*, Unieux-Firminy, France (NACE, Houston, Texas, 1973) p. 798.

10. B. G. Reisdorf, Trans. Am. Soc. Met., **56**, 783 (1963).

11. N. T. Thomas and K. Nobe, J. Electrochem. Soc. **117**, 622 (1970).

12. W. M. Robertson, Metall. Trans. **8A**, 1709 (1977).

13. M. Cornet, C. Bertrand, and M. Da Cunha Belo, Metall. Trans. **13A**, 141 (1982).

14. W. M. Robertson, Metall. Trans. **10A**, 489 (1979).

15. D. Webster, Trans. TMS-AIME, **242**, 640 (1968).

16. I. M. Bernstein and G. M. Pressouyre, in *Hydrogen Degradation of Ferrous Alloys*, R. A. Oriani, J. P. Hirth, and M. Smialowski, Eds., (Noyes Publications, 1985), p. 641.

17. N. R. Moody, M. W. Perra, and S. L. Robinson, in *Proceedings of the 4th International Conference on Hydrogen Effects on Material Behavior* (Moran, Wyoming, 1989).

18. M. T. Wang, Technical Rept. AFML-72-102, Part I (1972); Ref 105 in "The Stress Corrosion and Hydrogen Embrittlement Behavior of Maraging Steels", *Proceedings of the Conference on the Stress Corrosion Cracking and Hydrogen Embrittlement of Iron-Base Alloys*, Unieux-Firminy, France (NACE, Houston, Texas, 1973) p. 798.

19. W. Beck, J. O'M. Bockris, M. A. Genshaw, and P. K. Subramanyan, Metall. Trans. **2**, 883 (1971).

20. E. Lunarska-Borowiecka and N. F. Fiore, Metall. Trans. **12A**, 101 (1981).

21. S. Floreen, Metall. Rev. **13**, 115 (1968).

22. V. I. Sarrak, G. A. Filippov, and G. G. Kush, Phys. Met. Metall. **55**, 94 (1983).

23. M. Pressouyre, Metall. Trans. **10A**, 1571 (1979).

24. P. Lacombe, M. Aucouturier, J. P. Laurent, and G Lapasset, in *Proceedings of the Conference on Stress Corrosion Cracking and Hydrogen Embrittlement of Iron-Base Alloys*, Unieux-Firminy, France (NACE, Houston, Texas, 1973) p. 423.

25. M. Aucouturier, G. Lapasset, and T. Asaoka, Metallography **11**, 5 (1978).

26. G. R. Caskey, Mater. Sci. Engr. **14**, 109 (1974).

27. I. I. Phillips, P. Poole, and L. L. Shreir, Corros. Sci. **14**, 533 (1974).

28. A. E. Jenkins and H. W. Worner, J. Inst. Metal. **80**, 157 (1951/52).

29. H. Satoh, T. Fukuzuka, K. Shimogori, and H. Tanabe, in *Proceedings of the 2nd International Congress on Hydrogen in Metals*, (Paris, 1977).

30. R. J. Walter, R. P. Jewett, and W. T. Chandler, Mater. Sci. Engr. **5**, 98 (1969/70).

31. T. P. Groeneveld, E. E. Fletcher, and A. R. Elsea, "A Study of Hydrogen Embrittlement of Various Alloys," Summary Report, Contract No. NAS8-20029, NASA, MSFC, Huntsville, Alabama (1966).

32. C. G. Rhodes and A. W. Thompson, Metall. Trans. **8A**, 949 (1977).

33. R. W. Schutz and D. E. Thomas, in *Metals Handbook*, 9th ed., Vc 13, (ASM, Metals Park, Ohio, 1987), p. 669.

34. J. P. Stroup, A. H. Bauman, and A. Simkovich, Mater. Performance **15**, 43 (1976).

35. R. D. Kane, M. Watkins, D. F. Jacobs, and G. L. Hancock, Corrosion **33**, 309 (1977).